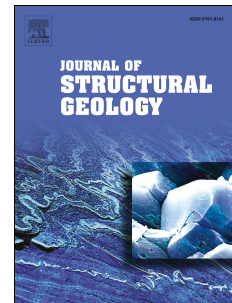


Accepted Manuscript

Structural data collection with mobile devices: Accuracy, redundancy, and best practices

Richard W. Allmendinger, Chris R. Siron, Chelsea P. Scott



PII: S0191-8141(17)30152-9

DOI: [10.1016/j.jsg.2017.07.011](https://doi.org/10.1016/j.jsg.2017.07.011)

Reference: SG 3507

To appear in: *Journal of Structural Geology*

Received Date: 12 May 2017

Revised Date: 19 July 2017

Accepted Date: 27 July 2017

Please cite this article as: Allmendinger, R.W., Siron, C.R., Scott, C.P., Structural data collection with mobile devices: Accuracy, redundancy, and best practices, *Journal of Structural Geology* (2017), doi: [10.1016/j.jsg.2017.07.011](https://doi.org/10.1016/j.jsg.2017.07.011).

This is a PDF file of an unedited manuscript that has been accepted for publication. As a service to our customers we are providing this early version of the manuscript. The manuscript will undergo copyediting, typesetting, and review of the resulting proof before it is published in its final form. Please note that during the production process errors may be discovered which could affect the content, and all legal disclaimers that apply to the journal pertain.

1 Structural data collection with mobile devices: 2 Accuracy, redundancy, and best practices

3 **Richard W. Allmendinger*, Chris R. Siron, and Chelsea P. Scott¹**

4 **Dept. of Earth and Atmospheric Sciences**

5 **Cornell University**

6 **Ithaca, NY 14850 USA**

7 Keywords: Smartphone, compass, orientation, accuracy, redundancy

8 Abstract

9 Smart phones are equipped with numerous sensors that enable orientation data collection
10 for structural geology at a rate up to an order of magnitude faster than traditional analog
11 compasses. The rapidity of measurement enables field structural geologists, for the first time, to
12 enjoy the benefits of data redundancy and quantitative uncertainty estimates. Recent work,
13 however, has called into question the reliability of sensors on Android devices. We present here
14 our experience with programming a new smart phone app from scratch, and using it and
15 commercial apps on iOS devices along with analog compasses in a series of controlled tests and
16 typical field use cases. Additionally, we document the relationships between iPhone
17 measurements and visible structures in satellite, drawing on a database of 3,700 iPhone
18 measurements of coseismic surface cracks we made in northern Chile following the Mw8.1
19 Pisagua earthquake in 2014. By comparing phone-collected attitudes to orientations determined
20 independently of the magnetic field, we avoid having to assume that the analog compass, which
21 is subject to its own uncertainties, is the canonical instrument. Our results suggest that iOS
22 devices are suitable for all but the most demanding applications as long as particular care is taken
23 with respect to metal and electronic objects that could affect the magnetic field.

*Corresponding author. Email address: rwa1@cornell.edu

¹ Now at: School of Earth and Space Exploration, Arizona State University, Tempe, AZ, USA

24 **1. Introduction**

25 Structural geology has always suffered from a relatively small number of recorded, quantitative
 26 measurements. A field geologist working with a traditional analog compass and paper field
 27 notebook typically records a few tens of orientation measurements per day. Not only are the total
 28 measurements small in number, but repeat measurements of sufficient quantity to establish
 29 statistical uncertainty are extremely rare in the published literature. Why bother to make tens of
 30 measurement of a single bedding surface at a single site when doing so would severely limit the
 31 number of outcrops we could document in a day? As Ramsay and Huber wrote with respect to
 32 strain measurements 35 years ago (Ramsay and Huber, 1983, p. 78), “it is often more rewarding
 33 to spend time in the field collecting a lot of data of relatively low degree of accuracy at many
 34 localities, rather than to concentrate on obtaining a few strain data with an extremely high degree
 35 of accuracy.” However, without data redundancy, it is impossible to evaluate the significance
 36 and accuracy of a measurement. Thus, the ideal case would be to make lots of measurements of
 37 high accuracy and well established uncertainty quickly enough that one can still visit many
 38 localities.

39 Smart phone compass/stereonet programs (“apps”) will very likely replace traditional
 40 analog compasses (Brunton, Freiberg, Silva, etc.) because of convenience, cost, and ubiquity but
 41 mostly because of their rapidity. The ability to record orientation along with location (latitude
 42 and longitude or UTM) and date/time with a single tap of an on-screen button reduces the
 43 amount of time that it takes to make a measurement. For timed tests on the same outcrop
 44 comparing analog compass and traditional paper note book to smart phone measurement and
 45 recording, the latter was about nine times faster. If many more measurements can be made in the
 46 same period of time, then field geologists can begin to enjoy the benefits of data redundancy that
 47 simply are not feasible with analog instruments. Additionally, in every cash-strapped geology
 48 department, the question will be, or is already being, asked: “why should we invest thousands of
 49 dollars in analog compasses when many students already have a smart phone at their disposal?”

50 The enthusiasm for smart phone orientation measurement apps was recently dampened
 51 somewhat by Novakova and Pavlis (2017) as well as earlier studies (e.g., Hama et al., 2014;
 52 Mookerjee et al., 2015) that demonstrate considerable variation in quality of device sensors and
 53 accuracy of recorded observation. Most conclude that the least reliable sensor is the device

54 magnetometer which likewise accords with our experience. However, comparisons in previous
 55 studies tend to be incomplete or misleading in assessment of accuracy because: only one
 56 operating system (i.e., Android or iOS) is tested, multiple devices are not used in testing, the
 57 details of the algorithms used in the apps are seldom well described, the error in the dip is
 58 assessed separately from the error in the strike (rather than using poles to planes; see section S1
 59 in the Supplementary Material), single measurements from analog compasses are regarded as
 60 canonical rather than comparing multiple analog compass measurements to multiple smart phone
 61 apps, and there is no assessment of accuracy that does not rely on the magnetic field.

62 Here, our purpose is three fold: (1) introduce a new, free iOS app, *Stereonet Mobile*,
 63 written by the senior author² and document the basics of its functioning; (2) compare *Stereonet*
 64 *Mobile* and a popular smart phone app, *Fieldmove Clino*, to each other and to analog compass
 65 measurements on a datum by datum and group by group basis; and (3) document the accuracy of
 66 app measurements independent of analog compass measurements by using a database of >3,700
 67 measurements of surface crack measurements and comparing those measurements with the same
 68 cracks visible on Google Earth imagery.

69 Our study, using only Apple® iPhones (iOS operating system), stands in contrast to
 70 Novakova and Pavlis (2017) who used only Android devices. Together, these two studies tend to
 71 suggest that the four different iPhones devices used here are significantly superior in accuracy
 72 and reliability compared to the two tested Android devices. This conclusion has also been
 73 reached by Midland Valley, the publisher of *Fieldmove Clino* who state, “We have observed
 74 much larger variations in the measured data recorded using Android devices which we suspect is
 75 largely down to the quality of the hardware components inside the device” (Midland Valley,
 76 2017). Our data are also consistent with the recent work of (Cawood et al., 2017) who compared
 77 remotely sensed surface data (LiDAR, Structure from Motion) to both digital and analog
 78 compass readings. However, anyone collecting irreplaceable field data with any electronic
 79 device will want to conduct their own tests and continue to carry an analog compass in the field
 80 with them. Even where a device is not reliable for data collection, many apps allow manual data

² Because *Stereonet Mobile* is available for free from the iOS App Store, the senior author has no financial conflict of interest.

81 entry, giving the user some of the benefits of the smart phone (e.g., automatic recording of
 82 location, time, and date) without the uncertainty in accuracy.

83 **2. Stereonet Mobile**

84 *2.1. Device Sensors*

85 Smart phones have a vast array of sensors to determine device orientation including GPS
 86 receivers, accelerometers, gyroscopes, magnetometers, and even barometers. From these sensors,
 87 it is possible to determine device orientation, position, velocity, and linear and rotational
 88 acceleration (Allan, 2011; Section S2 of the Supplementary Material). The iOS operating system
 89 provides the programmer with this derived information through its CoreMotion routines that
 90 handle the translation of the raw sensor data into the needed structural orientations. Foremost
 91 among these is magnetometer calibration that attempts to cancel out the effects of local magnetic
 92 fields, especially from other components within the device such as the power supply, etc., so that
 93 the orientation with respect to magnetic north can be determined. Dip measurements collected
 94 with smart phones are generally much more accurate than strikes because the magnetometer is
 95 much more sensitive to, and local perturbations more common in, the local magnetic field than in
 96 the local gravity field. The dip of the device can be determined from the three components of the
 97 acceleration due to gravity alone and does not have to depend on the magnetometer at all.

98 Sensors in the iPhone, sampled by the *Sensor Kinetics Pro* app at about 30 Hz, appear to
 99 be very stable (Fig. 1) especially in comparison to the Android devices tested by Novakova and
 100 Pavlis (2017, their figure 2). Nonetheless, the iPhone magnetometer is easily perturbed by
 101 passing even small metal objects within several centimeters of the device (Fig. 1b). This
 102 behavior has considerable implications for best practices in the field when using phones as data
 103 collection devices.

104 *2.2. Device Coordinate System and Determining Orientation*

105 The iOS device coordinate system and the rotations about the three axes are shown in
 106 Figure 2. One “reads” the face of the device like a right-handed map coordinate system: the first
 107 axis, X'_1 , is parallel to and in the short, or side-to-side, direction of the face with positive to the
 108 right. The second axis, X'_2 , is parallel to the face and the long axis of the device with positive

109 toward the top of the phone, and X'_3 , the third axis, is perpendicular to the face and positive
 110 towards the user. The change in orientations of the device is determined by the rotation of this
 111 coordinate system with respect to a reference coordinate system. The iOS operating system
 112 provides the programmer with four different potential reference frames. *Stereonet Mobile* uses
 113 the “CMAttitudeReferenceFrameXTrueNorthZVertical” reference frame. That is, the rotation
 114 matrix is equal to the identity matrix when the phone face is horizontal with the short axis (X'_1)
 115 aligned NS. To determine true north, the operating system must know the device position on the
 116 globe in order to calculate magnetic declination. Thus, reading an orientation must also turn on
 117 the device GPS receiver.

118 The change in orientation is supplied to the programmer by iOS in several different ways.
 119 Perhaps most common is using the Euler angles (Fig. 2), the pitch, roll, and yaw (sometimes
 120 known as the Tait-Bryan angles), which are familiar to anyone in aviation or boating.
 121 Determining device orientation using these angles, though, can be subject to an artifact known as
 122 gimbal lock where one degree of freedom is lost in certain orientations. Thus, iOS also provides
 123 orientation information via a rotation matrix or via quaternions. *Stereonet Mobile* uses the
 124 rotation matrix to calculate the orientation of the device relative to the reference frame. The
 125 rotation matrix, \mathbf{r} , in terms of the pitch roll and yaw, for iOS is given as:

$$\begin{aligned}
 r_{11} &= \cos(\text{roll})\cos(\text{yaw}) - \sin(\text{roll})\sin(\text{pitch})\sin(\text{yaw}) \\
 r_{12} &= \cos(\text{yaw})\sin(\text{roll})\sin(\text{pitch}) + \cos(\text{roll})\sin(\text{yaw}) \\
 r_{13} &= -\sin(\text{roll})\cos(\text{pitch}) \\
 r_{21} &= -\cos(\text{pitch})\sin(\text{yaw}) \\
 r_{22} &= \cos(\text{pitch})\cos(\text{yaw}) \\
 r_{23} &= \sin(\text{pitch}) \\
 r_{31} &= \cos(\text{roll})\sin(\text{pitch})\sin(\text{yaw}) + \cos(\text{yaw})\sin(\text{roll}) \\
 r_{32} &= \sin(\text{yaw})\sin(\text{roll}) - \cos(\text{roll})\cos(\text{yaw})\sin(\text{pitch}) \\
 r_{33} &= \cos(\text{roll})\cos(\text{pitch})
 \end{aligned}$$

127 The basic form of these equations will look familiar to anyone who has studied how rotations are
 128 accomplished in stereonet programs (e.g., Allmendinger et al., 2012) because they represent a
 129 single rotation accomplished by performing, in order, the three rotations about the three axes
 130 (i.e., three matrix multiplications).

131 The matrix, \mathbf{r} , is an orthogonal transformation matrix between the device coordinate
 132 system and the North-East-Down (NED) coordinate system familiar to structural geologists
 133 (because dips and plunges are measured with positive downwards). To translate device
 134 orientation to geological orientation, we simply calculate the orientation of a unit vector parallel
 135 to X'_3 (i.e., the pole to the device) for planes and another unit vector parallel to X'_2 , the long axis
 136 of the device, for lines (Fig. 2). In terms of direction cosines in a NED coordinate system, the
 137 pole to the phone and the geological surface against which it is held is given by:

$$\begin{aligned} \text{pole.north} &= r_{31} \\ \text{pole.east} &= -r_{32} \\ \text{pole.down} &= -r_{33} \end{aligned}$$

138

139 Likewise, a lineation's direction cosines are:

$$\begin{aligned} \text{lineation.north} &= r_{21} \\ \text{lineation.east} &= -r_{22} \\ \text{lineation.down} &= -r_{23} \end{aligned}$$

140

141 Because *Stereonet Mobile* uses the pole to the device, the user can place the back of the
 142 phone flush on the bedding surface in any orientation to measure the surface of interest. We have
 143 not noted any significant variation in accuracy when the phone is held in different positions,
 144 including upside-down. To measure a line, the long axis or edge of the phone must be parallel to
 145 the lineation on the rock but the back of the phone need not be flush against the rock. *Stereonet*
 146 *Mobile* can simultaneously measure the orientation of a plane and a line it contains by placing

147 the back of the phone flush on the rock with the long axis parallel to the lineation in the plane
 148 (Fig. 3a).

149 In cases where one would not want, or cannot, place the phone on the surface to be
 150 measured, *Stereonet Mobile* is also capable of measuring a plane's orientation by sighting
 151 through the device camera (Fig. 3b). When making a sighting measurement with the plane
 152 viewed edge-on, the pole to the device is assumed to be parallel to the strike direction and the
 153 long axis of the device parallel to the true dip direction. For sighting measurements made down-
 154 dip, the trend and plunge of the pole to the phone is assumed to be equal to the dip azimuth and
 155 dip of the plane.

156 *Stereonet Mobile* offers the user three planes formats to display planes data: strike and
 157 dip (using right-hand rule), dip azimuth and dip, or as poles. Nonetheless, internally it keeps
 158 track of all planes measurements in the first of the three formats.

159 2.3. *Redundant sampling*

160 Novakova and Pavlis (2017) demonstrated that, for Android devices, transients in the
 161 sensor data — brief marked excursions from the long term average value of the sensor — are a
 162 serious issue. While transients appear to be much less of an issue for iOS devices, *Stereonet*
 163 *Mobile* nonetheless uses oversampling to avoid any such problems. Before starting sampling,
 164 however, the device must be stable. *Stereonet Mobile* determines device stability using the
 165 acceleration and rotation rate data provided by the device. Absolute stability is not necessarily
 166 desirable as *Stereonet Mobile* permits the determination of orientation by sighting and, whenever
 167 the phone is not held against the rock, small motions are inevitable. Thus, stability in *Stereonet*
 168 *Mobile* is defined as user acceleration rates of $< 0.04 \text{ m/s}^2$ and rotation rates of $< 0.09 \text{ radians/s}$,
 169 values that were picked by trial and error. Stability constraints help to avoid inadvertent
 170 recording of data while the device is moving.

171 Once the user holds the device stably for 1 s, *Stereonet Mobile* determines the orientation
 172 every 100 ms and displays the mean and standard deviation of all measurements for as long as
 173 stability is maintained. For example, if the user holds the phone on a bedding surface for five
 174 seconds, the orientation and error displayed (Fig. 3) and recorded will reflect the average of 40
 175 measurements ((5 s - 1 s wait time) \times 10 samples/s). If the error in strike or dip exceeds 3° or the
 176 device is moved above the stability threshold, the values are deleted and averaging begins anew.

177 The same standards are used for lineation measurements and for measurements of planes by
 178 sighting with the device camera.

179 This sampling procedure is useful for eliminating random errors including sensor
 180 transients, but it does not eliminate systematic errors such as those that arise from the nearby
 181 environment. If the magnetic field is continuously perturbed by the presence of a nearby metal
 182 object, data redundancy will not fix the problem. The standard way to attempt to reduce such
 183 problems is by magnetometer calibration. For iOS devices, this is achieved by waving the phone
 184 in a figure-8 pattern or tilting and rotating the phone. In iOS 10 and with recent Apple® devices,
 185 one almost never sees the calibration screen, reflecting the increasing sophistication of the
 186 CoreMotion routines and services provided to the programmer. Nonetheless, in our experience,
 187 moving the phone in a figure-8 before starting measurements at a new outcrop or after making
 188 several measurements still seems to give better results than just assuming the operating system is
 189 giving the best possible orientations.

190 **3. Comparison to Analog Compass Readings**

191 In this section, we compare both *Stereonet Mobile* and *Fieldmove Cline* to measurements
 192 made by traditional analog compasses. An iPhone 6s and an iPhone 7, both running iOS 10.3
 193 were used for the digital measurements. Two traditional Brunton compasses, each a few decades
 194 old, were used to measure the strike of a plane and then the dip as separate measurements. A
 195 newer Brunton Geo compass was also used to measure dip azimuth and dip of planes in a single
 196 measurement, as one would do using a Freiberg compass. The traditional Brunton provides a
 197 more precise measure of dip than the Geo, simply because of the larger scale of the clinometer.
 198 Note that, for analog compasses, strike and dip are commonly independent measurements
 199 whereas the phone measures the pole to the plane in a single measurement.

200 **3.1. Controlled Test**

201 The first set of observations were collected in a highly controlled environment. A thin,
 202 heavy, flagstone of Archean Elba Quartzite from the Raft River Mountains of northwestern Utah
 203 measuring 96 by 53.5 cm was propped up at different angles in an outdoor setting away from
 204 environmental noise (e.g., power lines, metallic structures). Most of the surface roughness of the
 205 Elba is at a scale smaller than the area of the back of the compass or phone. The person making
 206 the measurements removed all metallic objects (keys, pocket knives, metallic wristwatches,

writing instruments, etc.). The quartzite slab was tilted at 72°, 45° and 30° and, for each dip orientation, we made 30 measurements each with *Stereonet Mobile*, with *Fieldmove Clino*, and with two types of Brunton compasses at different places on the slab (Fig. 4). Because there was no significant difference between the two types of analog compasses, those results were combined. No attempt was made to link individual measurements by different devices; instead, we wanted to calculate the best average determination of slab orientation. The actual number of individual measurements by *Stereonet Mobile* is much larger because each of the 30 measurements represents the average of many tens of measurements at 100 ms intervals.

Figure 4 depicts the results of this controlled test on an equal area, lower hemisphere projection. The α_{95} uncertainty cones for the mean vector of each individual group of 30 measurements vary from 0.4 to 0.6°. The angular difference between the mean vectors for each of the devices at each of the orientations is $\leq 2^\circ$. This difference is, in some cases, large enough that the uncertainty cones do not overlap. However, in a real world case, it is highly unlikely that a difference of $<2^\circ$ would make the slightest difference in all but the most demanding applications, in which case one would be unlikely to be using either an analog or digital compass!

The rose diagram (Fig. 4) shows the difference in strike between the different devices for the 72°-dipping data set. Although the measurements are not identical, the maximum of the strikes for the two iPhone apps and the analog compass measurements overlap. As shown in the Supplementary Material, as the dip decreases from 90°, the difference in strike becomes increasingly larger than the angular difference between the planes. Thus, the angular difference between poles should always be used for comparisons of measurements.

3.2. Field Test at Bear Valley, Pennsylvania

The Bear Valley strip mine (Fig. 5) in the Anthracite District of the Pennsylvania Valley and Ridge province is a classic locality (Nickelsen, 1979) visited by many generations of Northeastern U.S. geology students. The spectacular three-dimensional exposures of tightly folded Carboniferous strata are removed from power lines and metallic structures that might perturb the local magnetic field. We visited the site and collected comparative data using both *Stereonet Mobile* and traditional analog compasses in a typical field situation where no special attempt was made to remove metal objects from pockets, belts, etc. Because the site was stripped

237 to a single stratigraphic horizon, in many places in the pit, topographic contours lines —
 238 constructed from the Pennsylvania state LiDAR survey with a resolution of 2 ft (0.62 m) —
 239 parallel strike of the bedding. Thus, one can visually compare strikes measured at the site with
 240 local contours to assess accuracy of the iPhones; the fit is quite good in most cases. Two
 241 exceptions are at site 1, where the nose of an anticline was excavated to construct an access road,
 242 and locally where the device GPS mislocated the measurements by ~15 m (Fig. 5). In the latter
 243 case, the measurements were made in a narrow valley with limited sky view.

244 Two different types of studies were conducted. In the first, the same spot on the rock was
 245 measured both with *Stereonet Mobile* and with a Brunton compass, a plane-by-plane comparison.
 246 In the second, at three different sites, we measured ten strikes and dips using both the phone and
 247 the compass and, in one case, also using the sighting capability of *Stereonet Mobile*. Both
 248 experiments sampled rocks on both limbs of the folds, though not in the same place.

249 In the plane-by-plane comparison (Fig. 6), most measurements are close to each other but
 250 certainly not exactly the same. The median mismatch is 2.7° and average is $3.2 \pm 2.25^\circ$ with the
 251 distribution significantly skewed towards smaller angles (Fig. 6b). Four out of twenty-four
 252 measurements have mismatch angles exceeding 5.5° . While we presume that the analog compass
 253 measurements are more accurate, we have no independent means of verifying that assumption.
 254 Using the poles to bedding measured by the iPhone, the best-fitting fold axis as determined by
 255 the phone differs by just 0.1° from that determined by the analog compass. In other words, both
 256 data sets work equally well to determine the fold axis in these folded strata. Differences between
 257 phone and compass measurements lack consistency suggesting that the variations are random
 258 (Fig. 6, zoomed view).

259 In the second Bear Valley data set, average measurements of about 1 m^2 of three different
 260 bedding surfaces were determined (Fig. 7). In this case, while observations from iPhone and
 261 compass are very similar, the mismatch angles of the mean vectors of the poles ($3.5 - 4.3^\circ$) are
 262 slightly larger than the α_{95} uncertainty cones ($<2^\circ$). For the most gently dipping of the three
 263 bedding sites measured, the rose diagram (Fig. 7) shows that the strikes of the phone
 264 measurements appear consistently rotated clockwise by $5-10^\circ$, though the actual angular
 265 difference between the poles is less than 4° . If we calculate the fold axis from bedding poles
 266 determined from the iPhone measurements, the result differs by 4.4° with most of that difference

267 in the plunge angle. Although we do not know with great certainty the source of the mismatch
 268 between iPhone and compass measurements, the geologist who collected this data set was
 269 wearing a metal wristwatch, which can produce visible perturbations in the device magnetometer
 270 readings when held closer than 10 cm to the face of the phone (Fig. 1b).

271 **4. Independent Assessment of Phone Accuracy**

272 We generally assume that the analog compass is the canonical instrument and any
 273 deviation when compared with a phone measurement at the same locality indicates a deficiency
 274 of the phone. However, for any single phone-compass measurement pair, we have no
 275 independent means of verifying that the analog compass is more accurate. In this section, we
 276 compare a large number of iPhone measurements, not to compass measurements, but to the
 277 orientations of the structures visible on Google Earth imagery. The almost complete lack of
 278 vegetation in the Atacama Desert of northern Chile, combined with unique suites of surface
 279 cracks visible from space, make this comparison possible. Along with Chilean colleagues, the
 280 senior author and his students have been studying these surface cracks for the last 15 years
 281 (Baker et al., 2013; González et al., 2008; Loveless et al., 2005, 2009) and have mapped more
 282 than 50,000 individual crack traces on Google Earth and IKONOS imagery.

283 In 2014, the Mw8.1 Pisagua earthquake, located just offshore of northern Chile (Fig. 8),
 284 produced a new suite of fresh surface cracks which, in virtually all cases, reactivated the long-
 285 lived surface cracks visible on the satellite imagery (Fig. 9). The first and third authors
 286 documented the orientations of more than 3,700 fresh, coseismic cracks in 14 days of field work
 287 soon after the earthquake (Loveless et al., 2016; Scott et al., 2016). All of the original
 288 observations are available in the supplemental material associated with Scott et al. (2016). These
 289 new cracks were measured using an iPhone 4s and an iPhone 5s running the *Fieldmove Clino*
 290 app (*Stereonet Mobile* did not exist at that time). Of course, not all surface cracks were
 291 reactivated during the Pisagua earthquake so our measurements capture only a subset of the
 292 cracks visible from space. Nonetheless, this data set gives us a quantitative basis to compare
 293 phone-measured orientations with those visible in the imagery, independent of analog compass
 294 measurements. Though our iPhone measurements were checked periodically with analog
 295 compass measurements, it is unlikely that we would have been able to make 1/10th as many
 296 measurements without using the phones as primary data collection devices.

297 Because the surface cracks approximate vertical planes, the determination of the strike
 298 depends completely on the magnetometer and thus represents the best test of the most sensitive
 299 sensor of the phone (see also Section S1 of the Supplementary Material). The cracks, however,
 300 do have significant irregularities at various scales along strike (Fig. 9) such that measurement in
 301 the field necessarily involves some visual averaging, increasing the uncertainty of the
 302 measurement. Because uncertainty in location exists for any GPS receiver, commonly on the
 303 order of 5-10 m, we cannot always relate the orientation of every measured crack on the ground
 304 to those visible in satellite imagery. However, the spacing of the cracks is typically larger than
 305 the uncertainty in location of the phone measurements and thus a one-to-one correlation can be
 306 made surprisingly frequently. Finally, one should not expect perfect agreement between long-
 307 term cracks measured on satellite imagery and those fresh coseismic cracks measured on the
 308 ground: the latter constitute only a small subset of the former and at any particular site, only
 309 those cracks which were suitably oriented for reactivation opened coseismically.

310 We have chosen four sites out of the 72 visited to show here (Figs. 10-13). One can see
 311 the long-term cracks, in which the fresh coseismic cracks occur (Fig. 9a), clearly in the imagery
 312 at these four sites and they demonstrate well the relationship between coseismic crack
 313 orientations measured in the field using iPhones and the orientations of cracks in the imagery.
 314 For each site, we show both a satellite image with yellow lines parallel to the phone-measured
 315 strike of the coseismic cracks and a rose diagram comparing the long-term cracks on the imagery
 316 to the coseismic cracks measured with phones. All satellite images had some basic image
 317 processing, including contrast and tonal enhancement, sharpening, and denoising, to render them
 318 easier to see for publication. The statistics for each of the sites and data sets are summarized in
 319 Table 1.

320 For all sites, the circular mean of the coseismic crack orientation measured with phones is
 321 within about 10° of the mean of the long-term crack orientation measured on the imagery and, in
 322 all cases, the uncertainty ranges overlap at the 2σ level (Table 1). Furthermore, the azimuthal
 323 bins with the maximum number of strikes are identical in all but one case, even though the
 324 average reflects all orientations of the long-term cracks whereas the Pisagua earthquake cracks
 325 represent just a subset of the orientations at each site. This state is perhaps clearest at the Caleta
 326 Buena site (Fig. 11) where long-term cracks with azimuths between 045 and 090° are common
 327 but were not very suitably orientated for reactivation during the Pisagua earthquake. Likewise,

328 the Pampa de Tana site (Fig. 13) has numerous NNE to NS striking long-term cracks that were
 329 not reactivated.

330 The Punta de Lobos fan (Fig. 10) and the Caleta Junin (Fig. 12) sites have the most
 331 impressive correlation between long-term crack orientation as documented with satellite imagery
 332 and coseismic crack orientation measured with iPhones. Both visual inspection of the images, the
 333 rose diagrams, and the statistics all show that the iPhones captured the orientations very well.
 334 Thanks to a previous study at Punta de Lobos (Baker et al., 2013), we also have on-the-ground,
 335 long-term crack measurements made with a Brunton compass (Fig. 10). The Brunton
 336 measurements are statistically indistinguishable from the coseismic crack orientations measured
 337 with iPhones using *Fieldmove Clino*. Overall, these four sites are representative of the coseismic
 338 crack data set as a whole in terms of fidelity to local orientations.

339 **5. Discussion**

340 *5.1. Lessons pertinent to using iPhones as data collection devices*

341 In most cases, the angular mismatch between measurements made with several different
 342 iPhones and with traditional analog compasses or measurements on satellite imagery differ by
 343 less than 10°. In the case of the satellite imagery, the mismatch is probably much smaller than
 344 shown because of the inclusion of unreactivated, long-term cracks in the mean orientation
 345 calculation as reflected in the large and overlapping uncertainty intervals in the data sets (Table
 346 1). In places where one can with confidence visually relate field observations with specific
 347 cracks on the ground (e.g., Caleta Junin, Fig. 12), the correlation is surprisingly good. Overall,
 348 our 3,700 iPhone measurements in northern Chile provide robust proof that iPhones can be used
 349 in the field with good results.

350 The data from our controlled test using the Elba Quartzite flagstone (Fig. 4) at various
 351 dips demonstrates that iPhone measurements can be very reliable when appropriate precautions
 352 — removal of metal objects and electronics from the person making the measurements — are
 353 taken. When multiple measurements from the phone are averaged, they are just as good and
 354 nearly indistinguishable from a similar number of averaged measurements from traditional
 355 compasses. Both phone and compass have uncertainties and an average of analog measurements
 356 should be compared to an average of digital measurements.

357 No significant difference exists between the two iPhone programs tested, *Stereonet*
 358 *Mobile* and *Fieldmove Clino*, probably because both use the same iOS CoreMotion routines to
 359 calculate the orientation of the phone and thus the structure. *Fieldmove Clino* deployed on
 360 Android devices (Novakova and Pavlis, 2017) appears to be hostage to lower quality sensors.
 361 The iOS version performed very well in our northern Chile coseismic crack study. It is
 362 incumbent upon developers to explain how their software works to scientists who rely on their
 363 apps to collect priceless data. It would be useful to know, for example, what averaging schemes,
 364 if any, *Fieldmove Clino* uses and how it calculates orientation as we have done here with
 365 *Stereonet Mobile*.

366 The field test at Bear Valley (Figs. 5-7) likewise demonstrates that iPhones can be useful
 367 in a traditional field setting and, though perhaps not quite as accurate as analog compasses, can
 368 in aggregate provide useful information in a fraction of the time required to use the compass. The
 369 cylindrical fold axis determined by both phone and compass measurements from the same
 370 outcrops differs by less than 5°. The strikes also compare very well to contours of the LiDAR
 371 topography of the area (Fig. 5). The Bear Valley data set also highlights the Achilles heel of all
 372 smart phone measurements: the sensitivity of the device to local magnetic fields. In one case
 373 (Fig. 7), a systematic difference in strike of up to 10° may have been caused by the geologist's
 374 metal wristwatch that was reasonably close to the phone during measurement. However, even in
 375 that case, the actual angular difference between phone and analog compass measurements is less
 376 than 4°.

377 *5.2. Best practices for smart phone data collection*

378 The four different iPhones tested here are demonstrably superior for data collection to the
 379 two Android devices tested by Novakova and Pavlis (2017). This outcome suggests that anyone
 380 contemplating data collection with a smart phone should consider their device purchases very
 381 carefully, prioritizing quality and reliability over economy. However, on both platforms, phone
 382 components and operating systems change frequently and no one can guarantee absolutely that
 383 the most reliable phone today will be so two years from now. Unfortunately, most phone
 384 manufacturers have little incentive to make phones that are ideal for the structural geologist's
 385 purpose.

386 Regardless of the device purchased, one should always do careful tests similar to those
 387 described here to determine the reliability of their individual instrument before heading out to the
 388 field. General reputation of a manufacturer does not guarantee that the individual device will be
 389 adequate to the task. If a particular device proves faulty, many apps, including those described
 390 here, can still be used as data recorders, providing the user with automatic time, date, and
 391 location tagging of all observations.

392 When using a smart phone in the field, special care beyond that normally used with
 393 analog compasses should be taken around metal objects, magnets, and other electronic devices.
 394 For example, many phone cases have magnetic clips or closures that can thoroughly spoil your
 395 phone readings. Additionally, the user should be careful to remove from proximity seemingly
 396 innocent things like metal wristwatches, pens, hand lenses, pocket knives, tablets and laptops,
 397 etc.

398 Even though the magnetometer calibration screen seldom appears anymore in iOS 10, in
 399 our experience, it is a best practice to perform similar motions (figure-8s, tilting the phone in all
 400 orientations) before starting on any new outcrop. Additionally, similar calibrations should be
 401 undertaken periodically on a single outcrop or whenever a reading does not appear to make
 402 sense, or where digital and analog measurements differ significantly. Using a program that can
 403 display an orientation on a high-resolution satellite image so the user can verify that a
 404 measurement agrees with local geologic strike of the feature being measured can provide added
 405 confidence. Several field-based GIS systems, *Fieldmove Clino*, and the latest version of
 406 *Stereonet Mobile* can all do this.

407 It goes without saying that any phone being used for data collection should be protected
 408 from dust, water, and other abuse in a ruggedized, non-magnetic case. In some ways, data
 409 collection with a phone may actually be more secure than in a notebook: whenever the user has a
 410 cell or Wi-Fi signal, s/he can simply email the current data file to themselves. This facilitates
 411 back up of critical field data at more frequent intervals than one would do if they had to wait
 412 until returning to town to find a photocopy shop to copy one's field notes!

413 Standard field gear should include large capacity, rechargeable lithium ion batteries.
 414 Small, portable batteries with capacities exceeding 20,000 mAh cost less than \$50 and can
 415 recharge a smart phone completely 5-7 times. When we were using our phones to make 300 or

416 more measurements/day in Chile, the battery would become completely depleted at or even
 417 before the end of a ten hour field day. With 4 or 5 days between return trips into town, having
 418 such batteries available in one's camp and backpack is essential.

419 **6. Conclusions**

420 With some modest precautions, Apple® iPhones can be successfully used by structural
 421 geologists as data collection devices in the field. We have no direct experience with Android
 422 devices, but the work of Novakova and Pavlis (2017) is less encouraging for those devices. Both
 423 studies, however, tested an infinitesimally small number relative to the total number of devices
 424 that have been produced of each type and, furthermore, operating systems and device
 425 components change frequently. As of today, the structural geologist will still want to take their
 426 analog compass to the field with them and verify their phone observations. Anyone
 427 contemplating data collection with any smart phone needs to carry out extensive tests of the kind
 428 performed here to verify that the data collected are reliable.

429 When testing mobile devices, four best practices should apply: First, because both phone
 430 and analog compass measurements have uncertainty and natural surfaces are inherently irregular,
 431 one should make multiple measurement of the same surface using each type of instrument and
 432 compare the averages of the measurements. Comparing one-off measurements, as has commonly
 433 been done in the past, fails to acknowledge that uncertainty exists in all measurements with any
 434 type of instrument. Second, when evaluating planar orientations, one should always compare the
 435 angular difference between poles to the planes and not the difference in strike or dip. At low to
 436 moderate dips, the strike can differ significantly between two measurements even though the
 437 actual angular difference between the planes as determined by the poles is small. Third, the user
 438 should invest in a program that monitors the device sensors over time, note transients, and
 439 experiment with the effect of proximity of external metallic objects on the phone magnetometer.
 440 Several such apps are available for free or at modest cost in the app stores for both Android and
 441 iOS devices. Finally, where possible the user should compare their phone measurements, not
 442 only to analog compass measurements, but also to data independent of the magnetic field such as
 443 the LiDAR topographic contours (Fig. 5) and the Google Earth images (Figs. 10-13) used in this
 444 study.

445 Smart phones have already replaced compact cameras, video cameras, GPS receivers,
446 music players, digital voice recorders, exercise monitors, clinometers, and reference libraries. In
447 each of these cases, the question was not whether the phone was superior to the dedicated device
448 that it replaced but whether it was good enough for the purpose at hand. The results presented
449 here suggest that measuring orientations with iOS devices has achieved that status for all but the
450 most demanding applications. In most use cases, the accuracy of the iPhone is more than
451 sufficient given the variability of the natural feature being measured. Additionally, because the
452 rapidity and ease of use, iOS devices have a distinct advantage over analog compasses: multiple
453 measurements can be made rapidly and uncertainty instantly assessed. Making a single
454 measurement with an analog compass and paper field notebook is so time consuming that
455 geologists seldom make more than one measurement at a site and thus have no way to assess
456 uncertainty. Orientation data collection is entering the age of data redundancy and that is a good
457 thing.

458 **7. Acknowledgments**

459 The senior author thanks Paul Karabinos, Néstor Cardozo, and Haakon Fossen for beta
460 testing *Stereonet Mobile*. Comments from Fossen and Cardozo have helped to improve the
461 manuscript; Haakon reminded us of the Ramsay and Huber quote that appears in the first
462 paragraph. We are likewise grateful to Terry Pavlis and Steve Whitmeyer, and Editor William
463 Dunne for expert reviews of this manuscript though they may not necessarily agree with all of
464 the conclusions. The collection of the northern Chile field data was made possible by a RAPID
465 grant from the U.S. National Science Foundation, EAR-1443410.

466 **8. Appendix A. Supplementary Material**

467 Supplementary data and analyses related to this article can be found at
468 _____.

469 **9. References Cited**

- 470 Allan, A., 2011. Basic Sensors in iOS: Programming the Accelerometer, Gyroscope, and More, 1
471 ed. O'Reilly Media, Sebastopol, California, 108 p.
- 472 Allmendinger, R.W., Cardozo, N., and Fisher, D., 2012. Structural Geology Algorithms: Vectors
473 & Tensors, ed. Cambridge University Press, Cambridge, England, 289 p.
- 474 Baker, A., Allmendinger, R.W., Owen, L.A., and Rech, J.A., 2013. Permanent deformation
475 caused by subduction earthquakes in northern Chile. *Nature Geoscience* 6, 492-496.
- 476 Cawood, A.J., Bond, C.E., Howell, J.A., Butler, R.W.H., and Totake, Y., 2017. LiDAR, UAV or
477 compass-clinometer? Accuracy, coverage and the effects on structural models. *Journal of*
478 *Structural Geology* 98, 67-82.
- 479 González, G., Gerbault, M., Martinod, J., Cembrano, J., Allmendinger, R., Carrizo, D., and Espi-
480 na, J., 2008. Crack formation on top of propagating reverse faults of the Chuculay Fault
481 System northern Chile: insights from field data and numerical modeling. *Journal of*
482 *Structural Geology* 30, 791-808.
- 483 Hama, L., Ruddle, R.A., and Paton, D., 2014. Geological Orientation Measurements using an
484 iPad: Method Comparison. *TPCG*, 45-50.
- 485 Loveless, J.P., Allmendinger, R.W., Pritchard, M.E., Garway, J.L., and González, G., 2009.
486 Surface cracks record long-term seismic segmentation of the Andean margin. *Geology*
487 37, 23-26.
- 488 Loveless, J.P., Hoke, G.D., Allmendinger, R.W., González, G., Isacks, B.L., and Carrizo, D.A.,
489 2005. Pervasive cracking of the northern Chilean Coastal Cordillera: New evidence of
490 forearc extension. *Geology* 33, 973-976.
- 491 Loveless, J.P., Scott, C.P., Allmendinger, R.W., and González, G., 2016. Slip distribution of the
492 2014 $M_w=8.1$ Pisagua, northern Chile, earthquake estimated from coseismic fore-arc sur-
493 face cracks. *Geophysical Research Letters* 43, 10134-10141.
- 494 Midland Valley, 2017. Fieldmove clino: Android users guide, ed. Midland Valley, Glasgow,
495 Scotland, 38 p.
- 496 Mookerjee, M., Vieira, D., Chan, M., Gill, Y., Pavlis, T. L., Spear, F., and Tikof, B., 2015. Field
497 data management: Integrating cyberscience and geoscience. *Eos* 96, 18-21.
- 498 Nickelsen, R.P., 1979. Sequence of structural stages of the Alleghany Orogeny, at the Bear Val-
499 ley strip mine, Shamokin, Pennsylvania. *American Journal of Science* 279, 225-271.
- 500 Novakova, L., and Pavlis, T.L., 2017. Assessment of the precision of smart phones and tablets
501 for measurement of planar orientations: A case study. *Journal of Structural Geology* 97,
502 93-103.
- 503 Ramsay, J.G., and Huber, M.I., 1983. The techniques of modern structural geology, volume 1:
504 Strain analysis, ed. Academic Press, London, 307 p.
- 505 Scott, C.P., Allmendinger, R.W., González, G., and Loveless, J.P., 2016. Coseismic extension
506 from surface cracks reopened by the 2014 Pisagua, northern Chile, earthquake sequence.
507 *Geology* 44, 387-390.

508 **9. Figure Captions**

509 Figure 1. Graphs showing sensitivity of (a) orientation, (b) magnetometer, and (c)
 510 accelerometer sensors on one of the iPhones used in this study. The sensors were sampled at ~30
 511 Hz using the *Sensor Kinetics Pro* app available in the iOS app store. Compare this figure to
 512 Figure 2 of Novakova and Pavlis (2017). In each, green corresponds to the X1 axis, blue to the
 513 X2 axis, and red to the X3 axis (see Figure 2 for the coordinate system). The inset diagrams
 514 magnify the graph to show the variability of the sensor data. In (b), the device magnetometer was
 515 perturbed by passing a metal object ~5 cm from the device at the times indicated.

516 Figure 2. The iOS device coordinate system (X'_1, X'_2, X'_3) and its relationship to a typical
 517 structural geology North-East-Down (X_1, X_2, X_3) coordinate system. Device orientation is
 518 determined by transforming the unit vectors \hat{p} and \hat{l} into the unprimed geographic coordinate
 519 system. Selected direction cosines of the transformation matrix are shown. Many programs use
 520 the Euler angles pitch, roll, and yaw to determine device orientation but iOS also provides the
 521 programmer with access to the rotation matrix and quaternions. *Stereonet Mobile* uses the
 522 former.

523 Figure 3. Screen captures of *Stereonet Mobile* in data capture mode. (a) Data capture by
 524 placing the device directly on the rock surface to be measured. The app is capable of capturing
 525 both the plane and a line in the plane in a single measurement. (b) Data capture by sighting
 526 parallel to the strike direction using the device camera. The green circle in the lower right shows
 527 that the direction of sight (pole to the phone) is within 2° of horizontal. In both cases, once stable
 528 the phone measures the orientation of the device every 100 ms and reports the uncertainty to the
 529 user.

530 Figure 4. Controlled experiment using a flagstone of Elba Quartzite propped up at
 531 different angles. Thirty measurements each were made using the two smart phone apps, *Stereonet*
 532 *Mobile* and *Fieldmove Clino*, and two different analog compasses, a traditional Brunton and a
 533 Brunton Geo. The difference in mean vector (large circles show error cones) of the poles to the
 534 plane (small dots) for the three different dips are shown graphically and numerically. Zoomed in
 535 views in lower right show the α_{95} confidence cones for each of the three instruments at each of
 536 the three dips. Petals in all rose diagrams in this and subsequent figures are filled with alpha

537 channel transparency so that the reader can see where more than one petal overlaps. Additional
 538 apparent colors are due to overlapping primary colors and partial transparency.

539 Figure 5. Topographic map of part of the abandoned open pit at Bear Valley,
 540 Pennsylvania. Topographic contours constructed from the Pennsylvanian state LiDAR data set,
 541 originally at 2 ft. (0.62 m) intervals. For clarity, only 10 ft. (3.05 m) contours are shown. Because
 542 the pit was stripped to a single stratigraphic horizon, contour lines should approximate strike of
 543 bedding in many parts of the pit, though not at Site 1. The red strikes and dips were measured
 544 with an iPhone 7 and are plotted on the stereonet in Figure 6; the blue strikes and dips were
 545 measured with an iPhone 6s and plotted in Figure 7; additional strikes and dips shown in black.
 546 Locations generally have uncertainties of ± 5 to ± 10 m. All sites also have analog compass
 547 measurements but those data are not plotted here.

548 Figure 6. Measurement by measurement comparison of *Stereonet Mobile* and Brunton
 549 compass measurements at Bear Valley, Pennsylvania. (a) Both poles (dots) and planes (great
 550 circles) are shown. The arcs in the zoomed in views on the left connect each analog compass
 551 measurement (in red) with the corresponding phone measurement (in black). Although most of
 552 the difference is in the strike value, there is no consistent difference. In some cases the phone
 553 measurement is rotated clockwise and in other cases counter clockwise with respect to the
 554 compass measurement. Difference between the calculated fold axis from the two different data
 555 sets is 0.1° . (b) Histogram of the angular mismatch of poles to planes between phone and
 556 compass for each of the 24 measurements in (a).

557 Figure 7. Ten phone and ten Brunton measurements of three different irregular bedding
 558 surfaces, showing planes (great circles) and poles (dots) as well as mean vectors and α_{95}
 559 uncertainty cones for each population. The delta angles are the difference of the mean vectors of
 560 each population at each site. For the lowest dipping strata, ten measurements of bedding using
 561 *Stereonet Mobile*'s sighting routine were also made (blue great circles). The rose diagram of
 562 strike directions shown for the lowest dipping site indicate that the phone strikes are rotated
 563 clockwise from the Brunton Geo strikes by about $5\text{--}10^\circ$, although the angular difference of the
 564 poles are just 3.7° .

565 Figure 8. Map of Pisagua earthquake and location of the four sites depicted in Figures 10-
 566 13 depicted with large yellow stars. Locations of the main shock as well as a significant

567 foreshock and aftershock are shown. The colored “butterflies” show the average and 2σ
 568 uncertainty of crack orientations at each of the 72 sites studied. See Scott et al. (2016) and
 569 Loveless et al. (2016) for more information.

570 Figure 9. Typical coseismic cracks produced during the Pisagua earthquake. (a) A long-
 571 term crack filled with aeolian sand (marked by white arrows) showing fresh reactivated cracks in
 572 the middle. (b) Detail of a fresh coseismic crack cutting across faintly visible tire tracks.

573 Figure 10. Punta de Lobos fan surface (Baker et al., 2013) shown in a Google Earth
 574 image and the locations and orientations of coseismic cracks, measured with phones in the field,
 575 shown as short yellow line segments along three transects. Circular histogram (rose diagram)
 576 shows the orientations of all long-term cracks measured on the imagery along the transects (red
 577 petals), long-term cracks measured with Brunton compass (green petals) and the orientations of
 578 coseismic cracks measured with iPhones (blue petals). There is no significant difference between
 579 iPhone and Brunton measurements. The mean vector for the imagery-measured cracks captures a
 580 small population of NW-striking long-term cracks that were not reactivated during the
 581 earthquake. Coordinates of image center are: 21.03846°S, 70.123084°W.

582 Figure 11. Caleta Buena site. The Pisagua earthquake preferentially reactivated the NW-
 583 striking cracks at this area, with only very minor reactivation of the prevalent NE-striking long-
 584 term cracks. Yellow line segments are strikes of coseismic cracks measured with phones in the
 585 field. Coordinates of image center are: 19.895783°S, 70.077480°W.

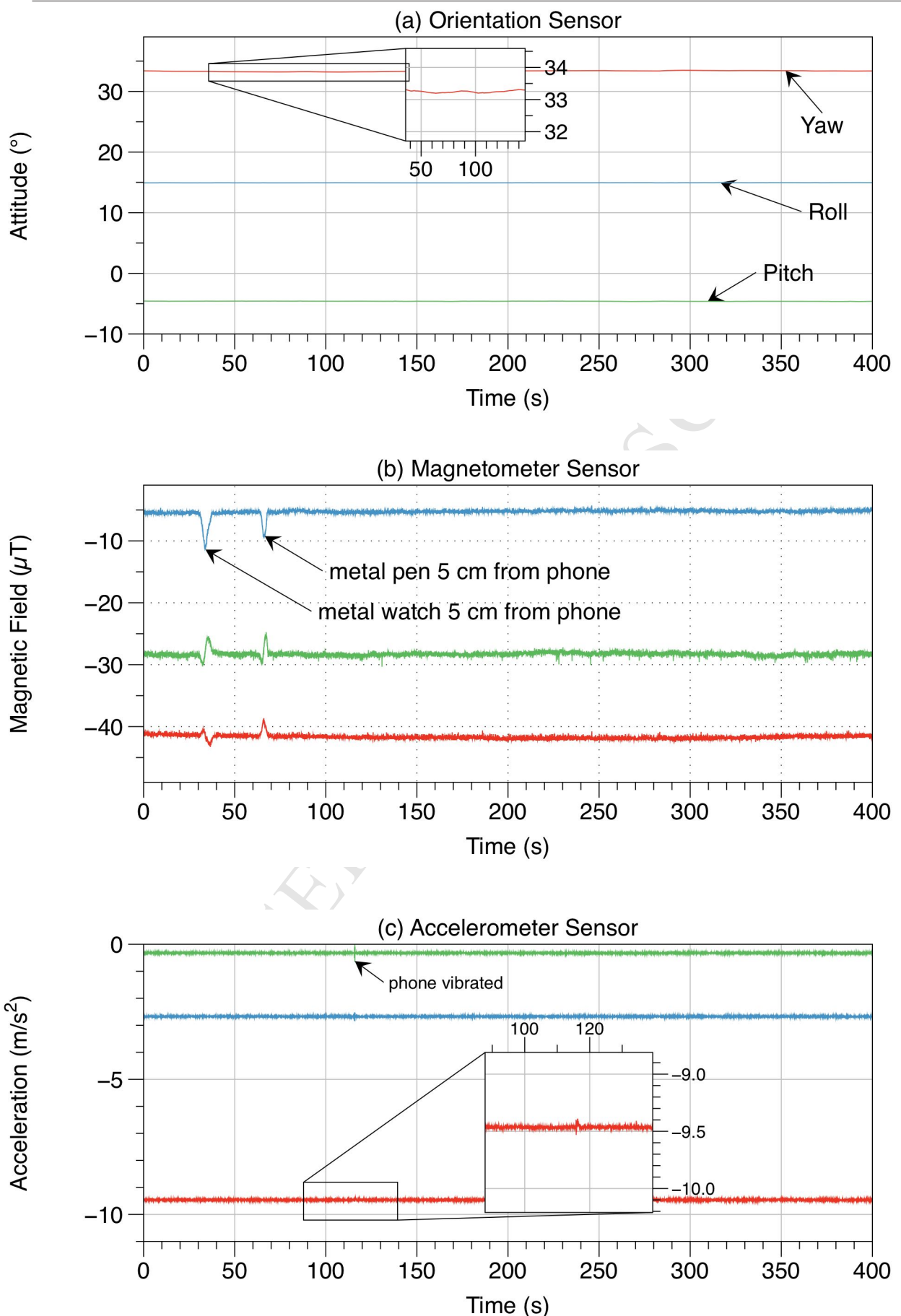
586 Figure 12. Caleta Junin site, located close to the epicenter of the Pisagua earthquake.
 587 Correlation of long-term cracks mapped on Google Earth and coseismic cracks measured with
 588 iPhones is particularly good at this site as the long-term cracks are relatively unimodal and were
 589 well-oriented for reactivation during the earthquake. Yellow line segments are strikes of
 590 coseismic cracks measured with phones in the field. Coordinates of image center are:
 591 19.692243°S, 70.128908°W.

592 Figure 13. Pampa de Tana site showing preferential reactivation of the WNW-striking
 593 long-term cracks and relatively infrequent reactivation of the prominent, though secondary, ~NS-
 594 oriented cracks. Yellow line segments are strikes of coseismic cracks measured with phones in
 595 the field. Coordinates of image center are: 19.401761°S, 70.137968°W.

596 **Table 1.**

		Punta de Lo-bos	Caleta Buena	Caleta Junin	Pampa de Tana
mean vector & 2σ uncertainty	long-term image	$354.1 \pm 7.1^\circ$	$313.6 \pm 25.3^\circ$	$347.8 \pm 19.0^\circ$	$297.0 \pm 9.2^\circ$
	long-term Brunton	004.3 ± 4.9	N/A	N/A	N/A
	coseismic	$006.9 \pm 9.2^\circ$	323.1 ± 16.3	352.6 ± 12.5	$286.3 \pm 12.3^\circ$
Bin azimuth w/ max count	long-term	001 - 010°	331 - 340°	351 - 360°	281 - 290°
	long-term Brunton	001 - 010°	N/A	N/A	N/A
	coseismic	001 - 010°	321 - 330°	351 - 360°	281 - 290°

597



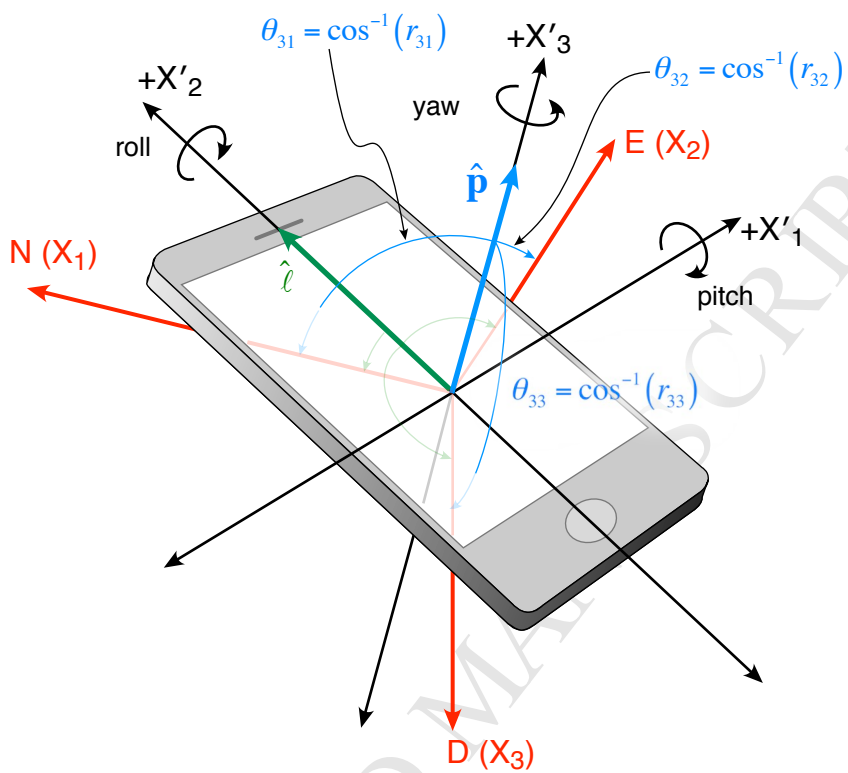
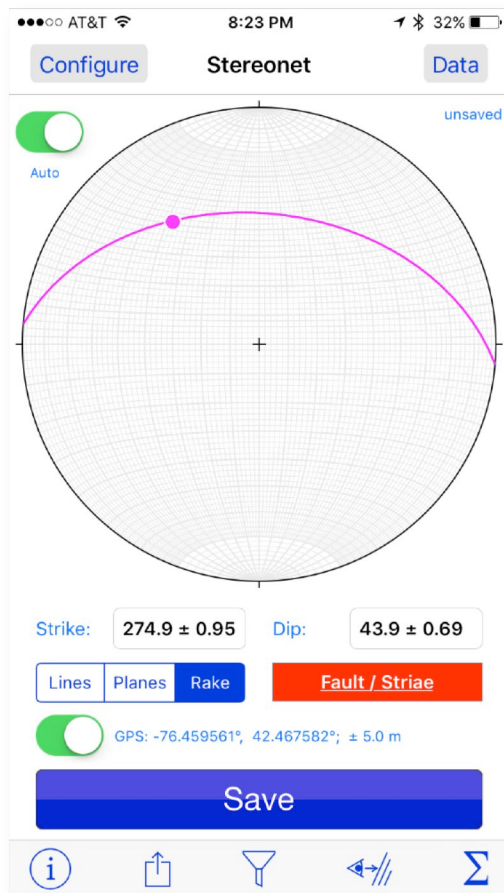


Fig. 2

(a) Stereonet view



(b) Sighting view



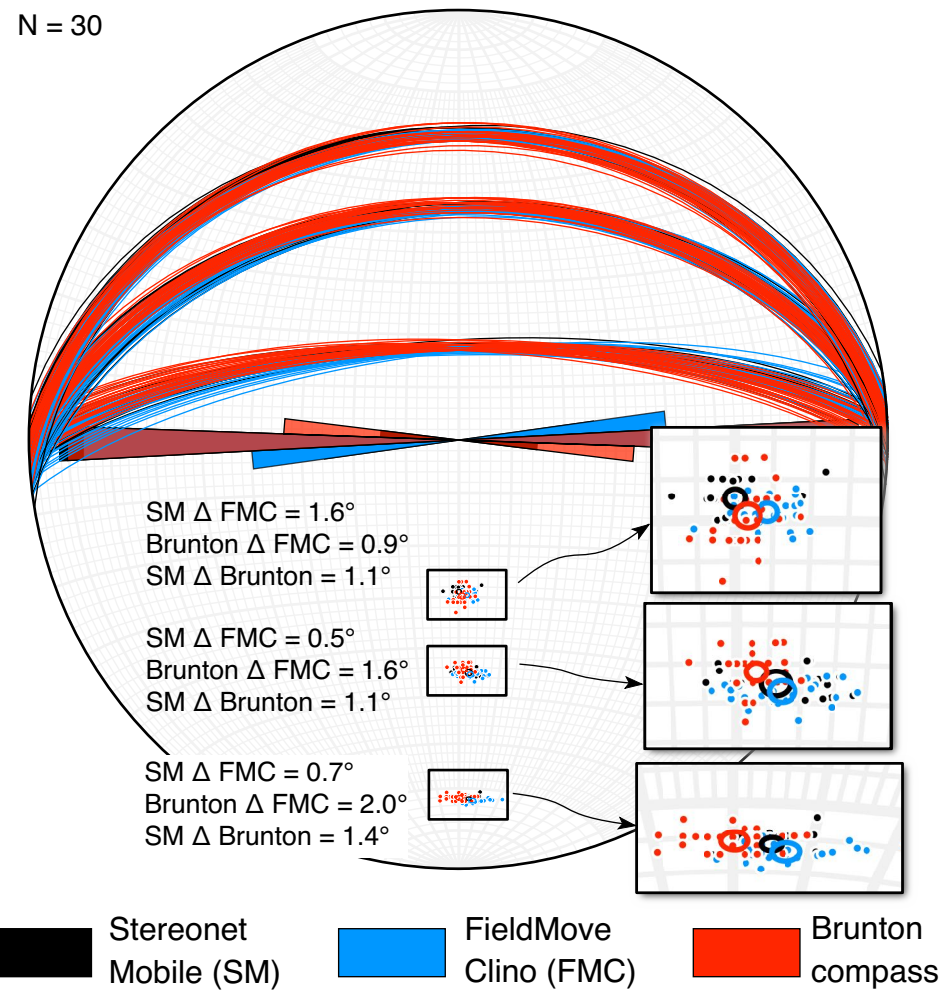


Fig. 4

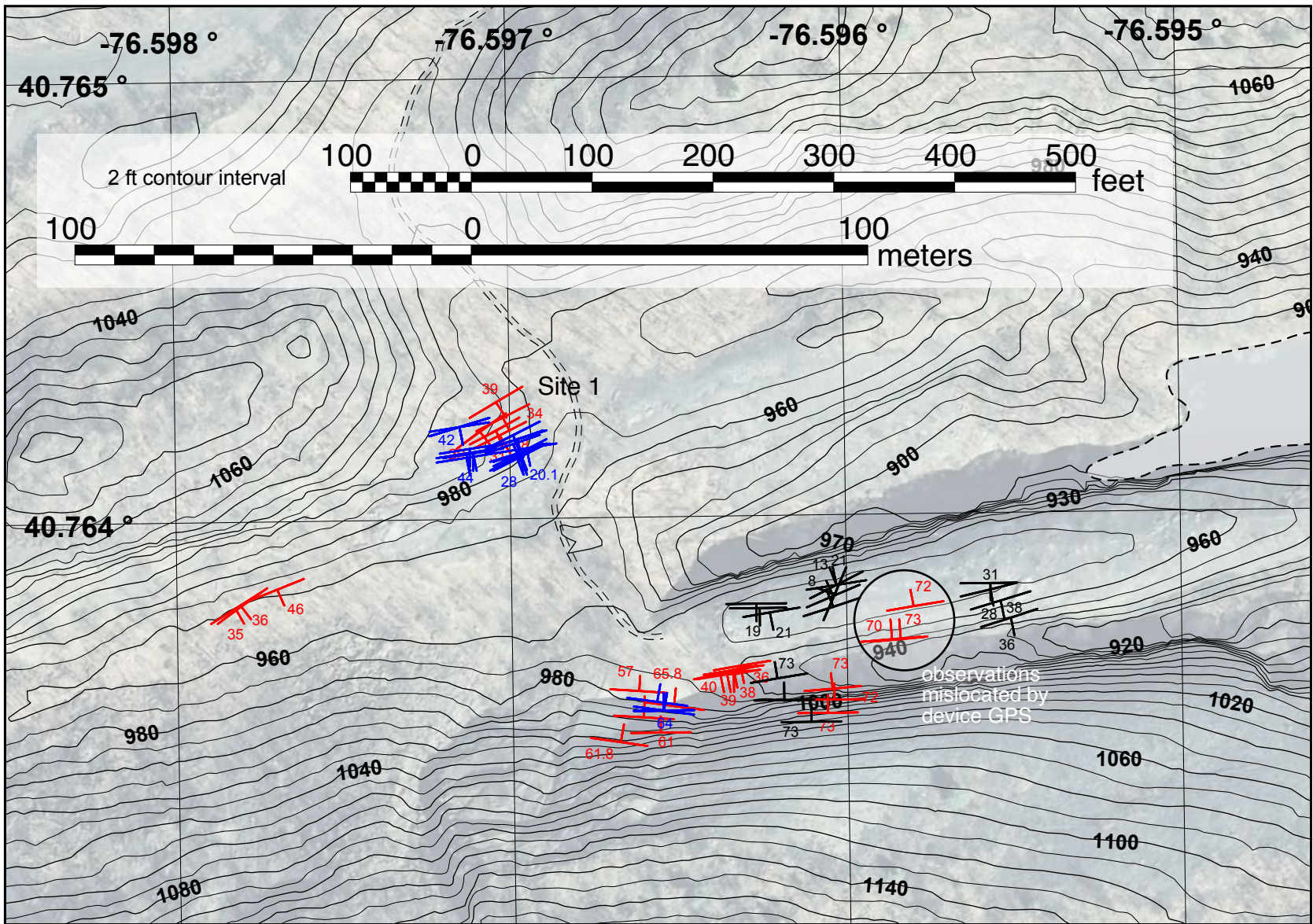


Fig. 5

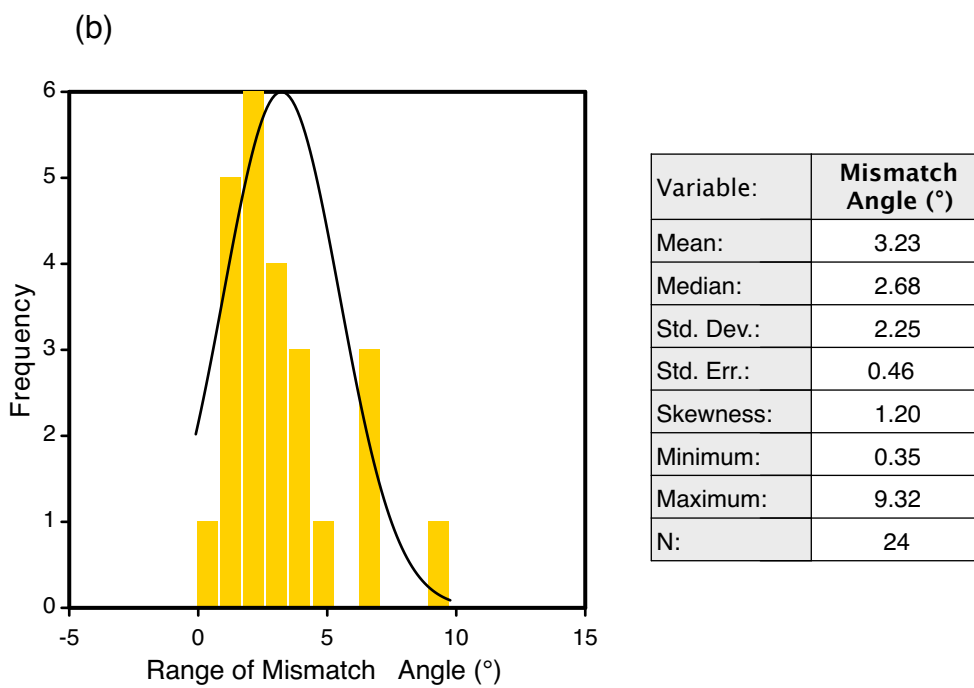
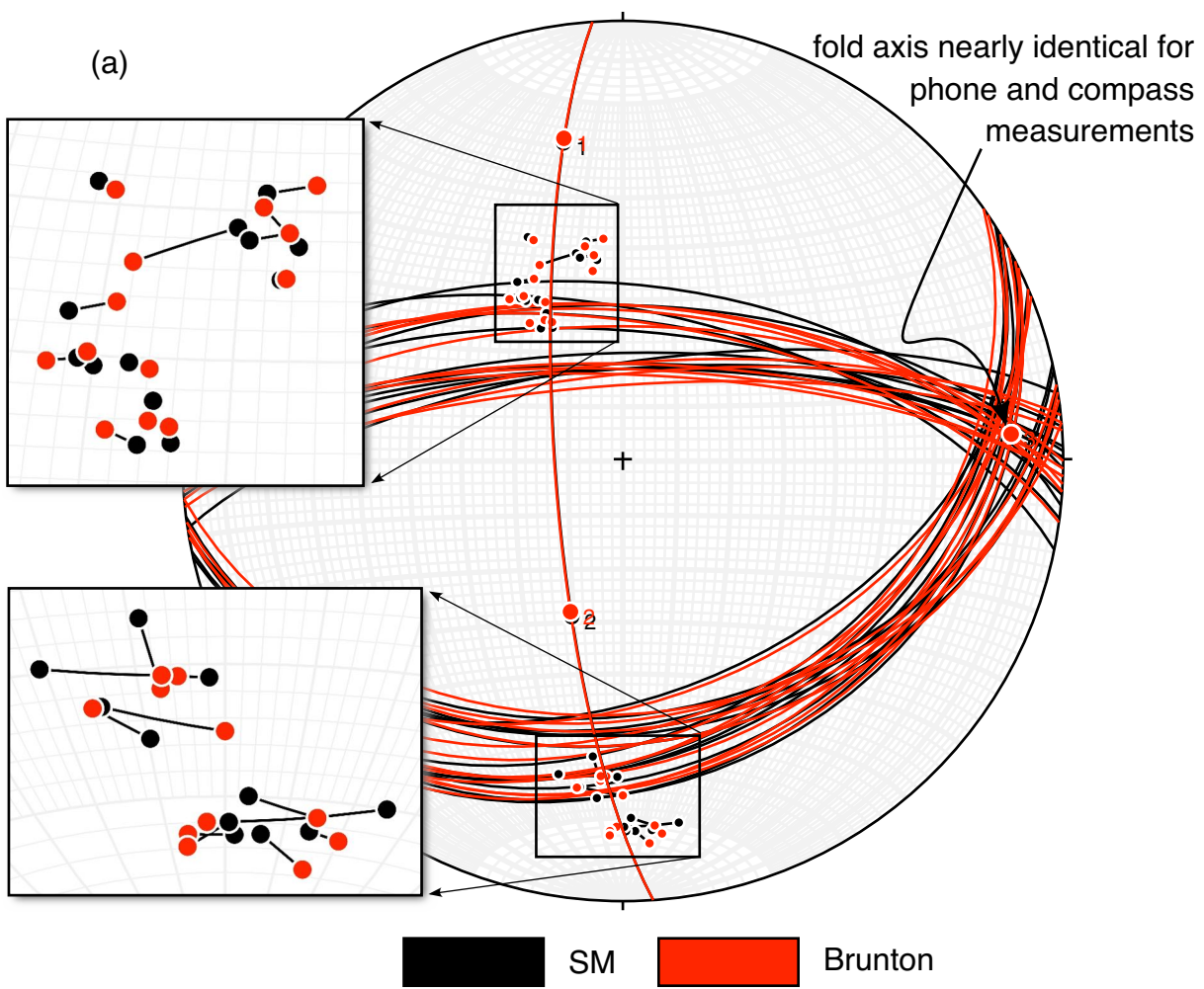


Fig. 6

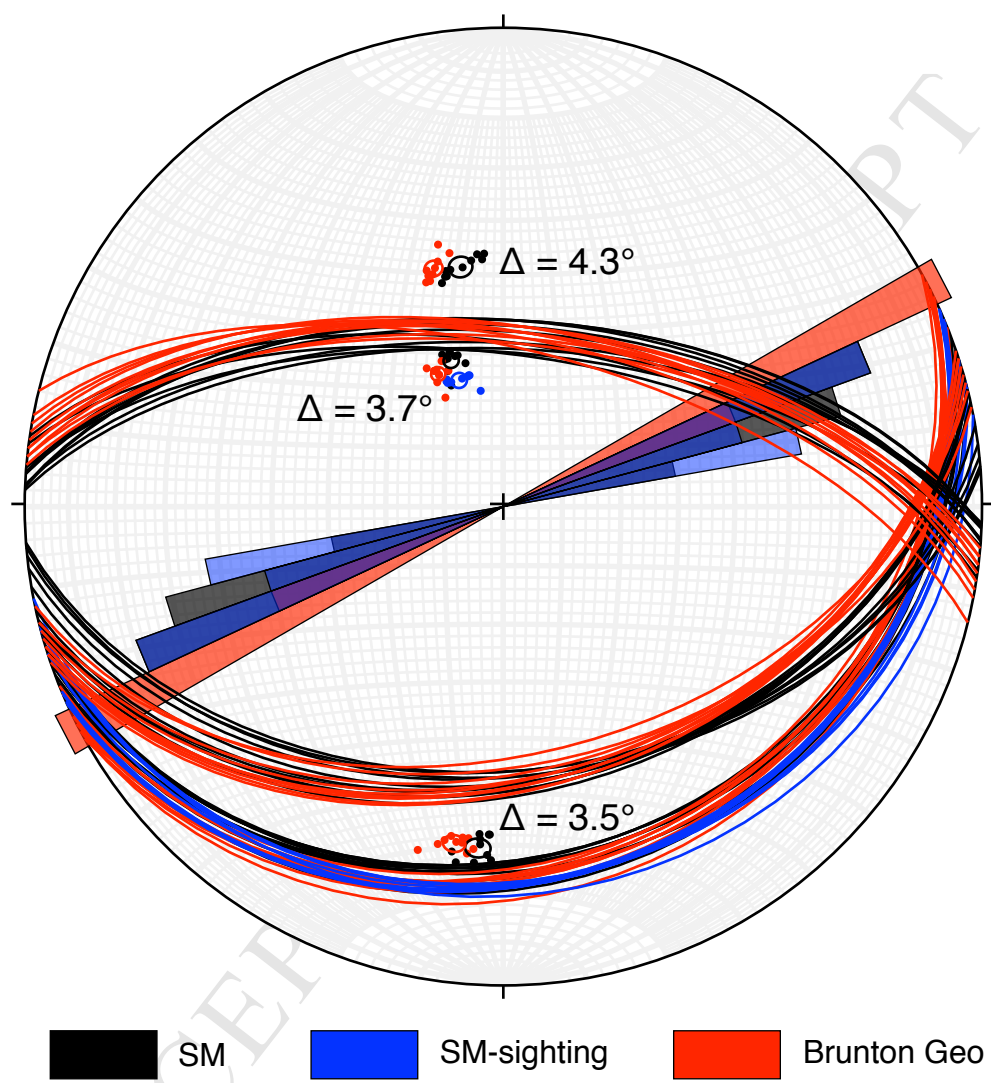


Fig. 7

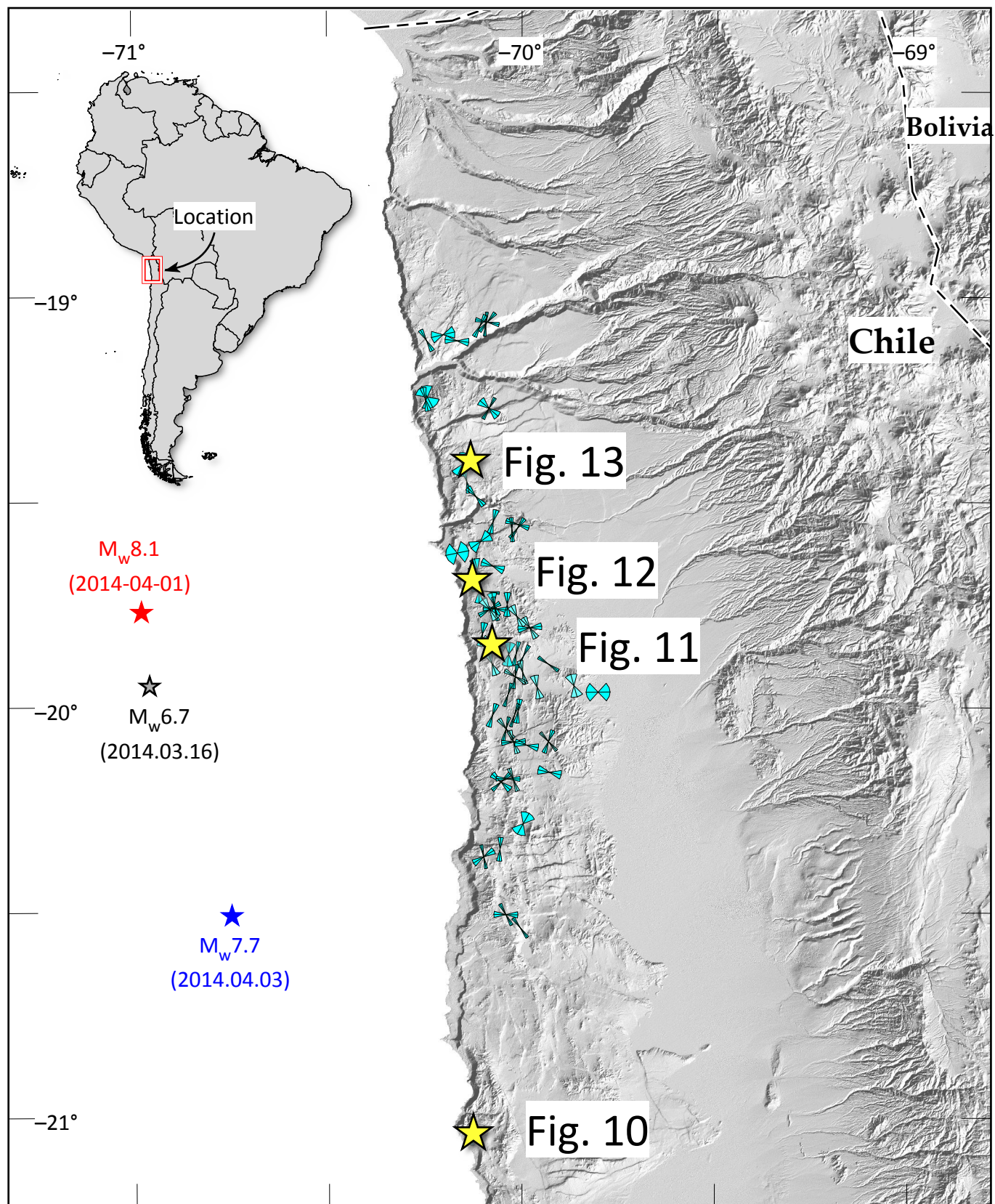


Fig. 8

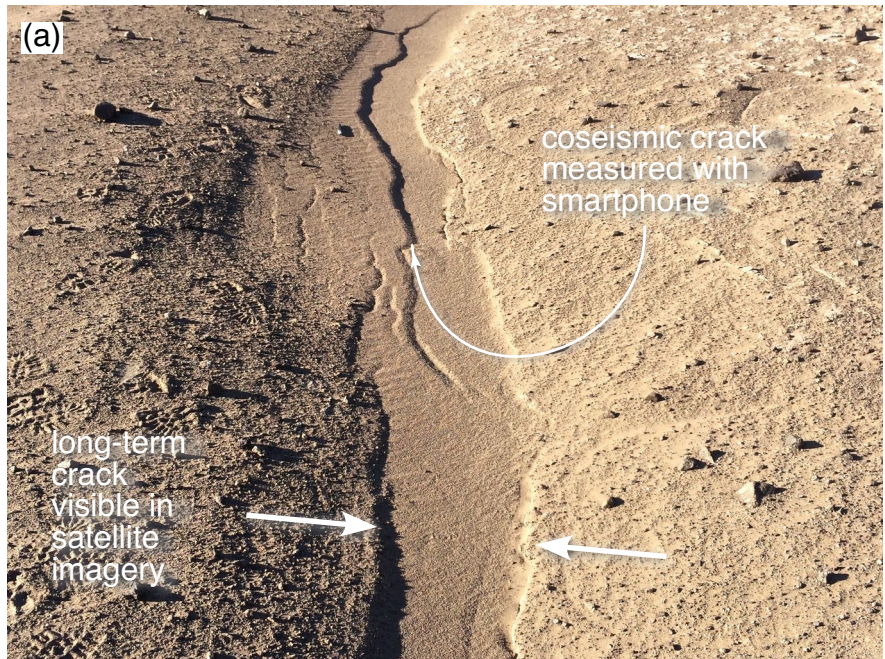


Fig. 9

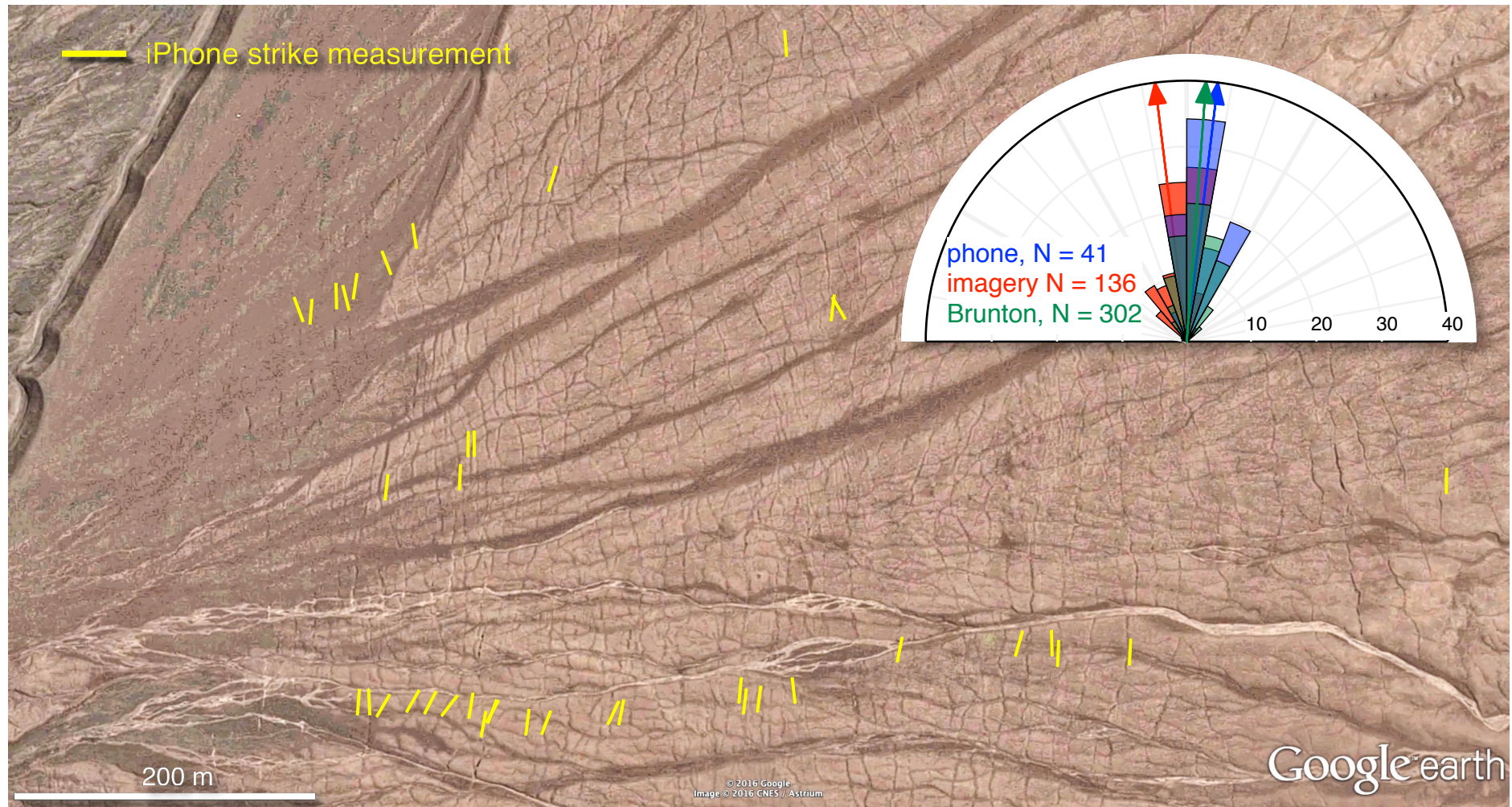


Fig. 10

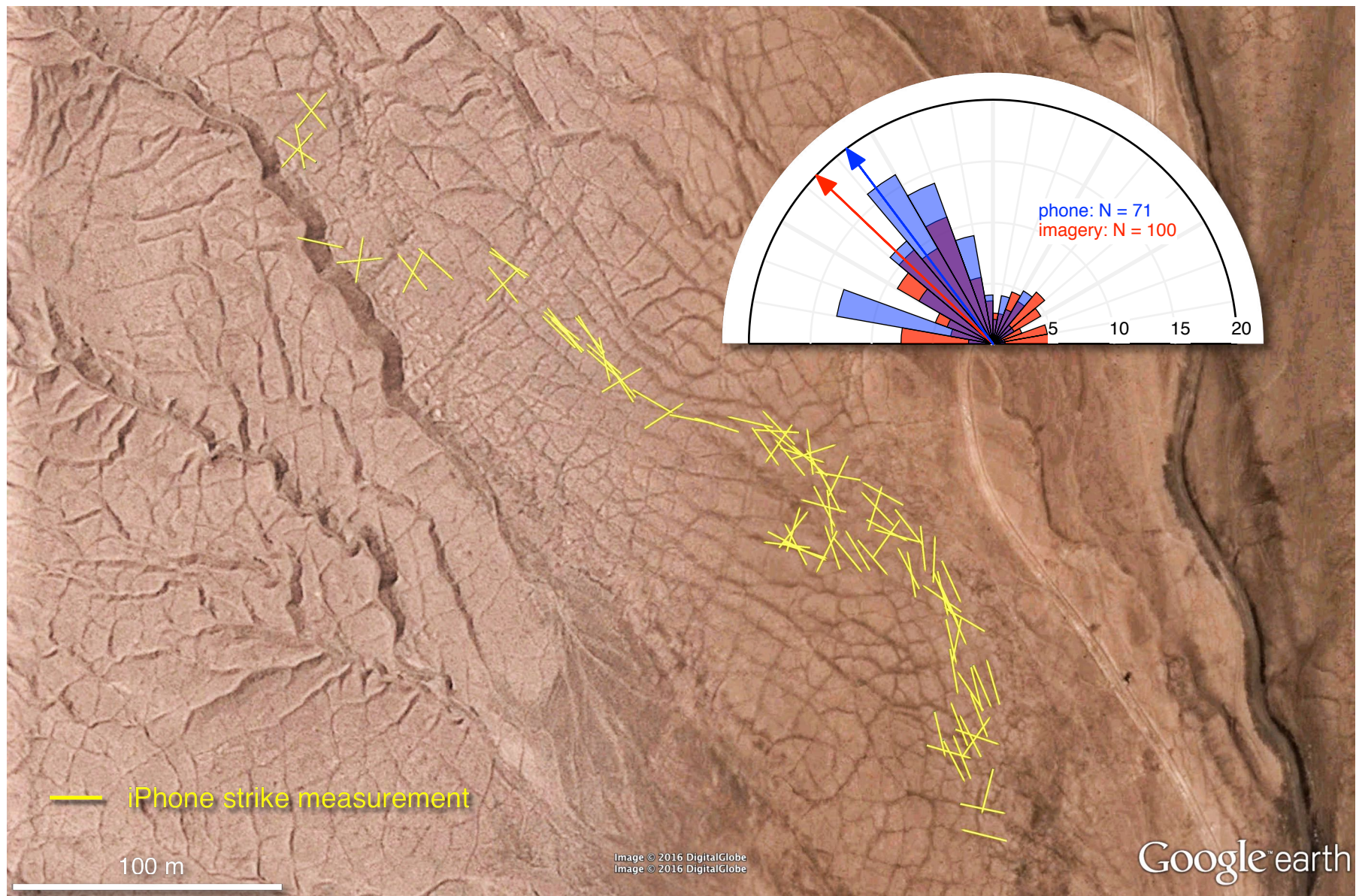


Fig. 11

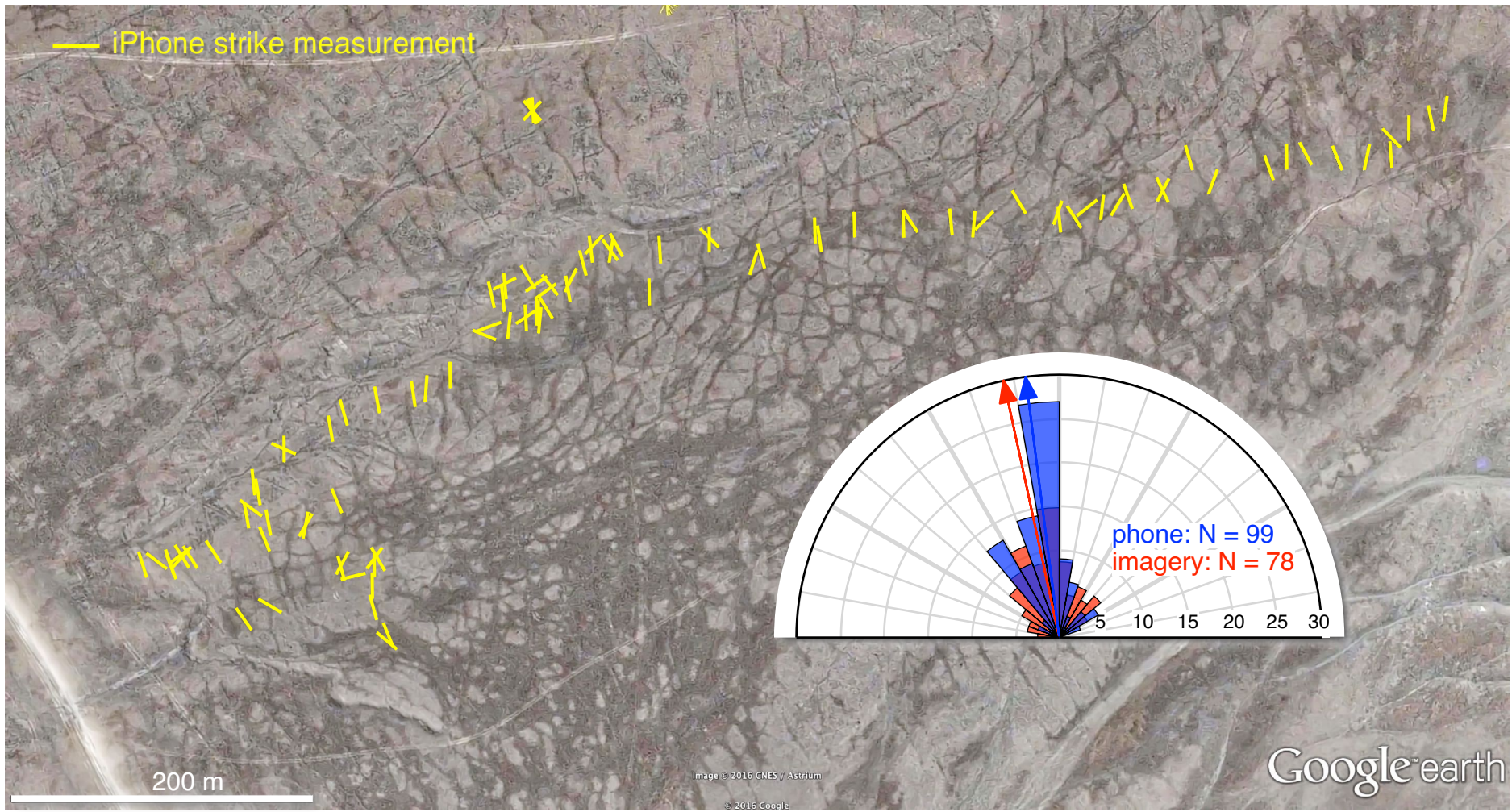


Fig. 12

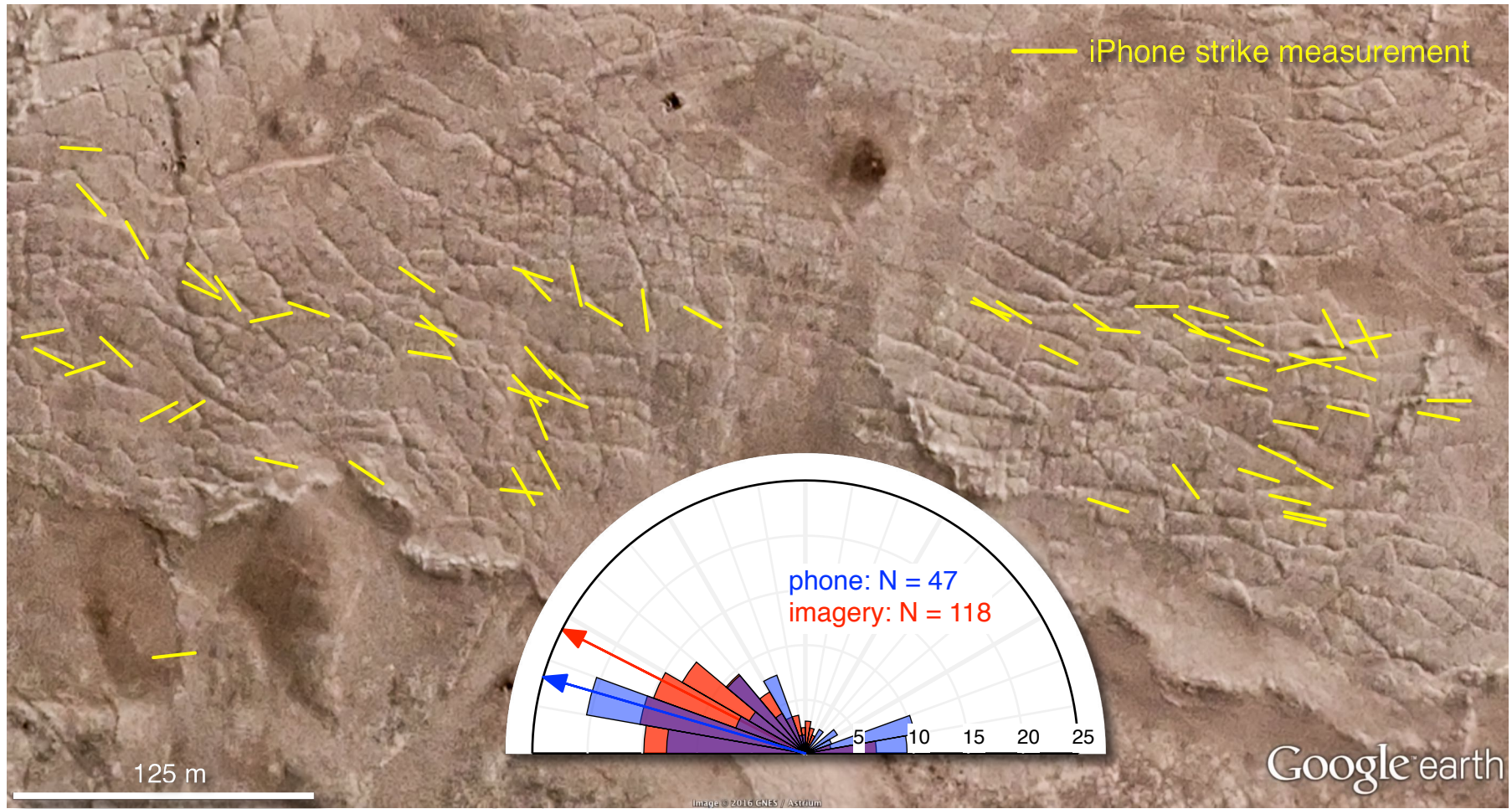


Fig. 13

Highlights

- The accuracy of iOS devices is sufficient for structural geology data collection tasks
- Accuracy determined independent of analog compass measurements
- iOS device measurements compare well to analog compass measurements
- A new iOS compass/stereonet app is described